Rev. Roum. Sci. Techn.– Électrotechn. et Énerg.
Vol. 61, 2, pp. 142–146, Bucarest, 2016

SLIDING MODE DIRECT TORQUE AND ROTOR FLUX CONTROL OF AN ISOLATED INDUCTION GENERATOR INCLUDING MAGNETIC SATURATION

ADEL ABERBOUR[1], KASSA IDJDARENE[1], ABDELMOUNAÏM TOUNZI[2]

Key words: Direct torque and rotor flux control (DTRFC), Sliding mode control, Autonomous induction generator, Magnetic saturation.

This paper presents a control system of an isolated squirrel cage induction generator (IG), whose stator windings are connected to a PWM inverter/rectifier, using direct torque and rotor flux control (DTRFC) algorithm based on the sliding mode approach. Unlike the conventional vector control scheme, the proposed control strategy permits to directly control the flux and torque without resorting to the usually used current control loops. The three phase induction generator is modeled through a diphase approach and the magnetic saturation phenomenon is included both in the IG model and in the control algorithm via a variable magnetizing inductance, based on experimental tests. The control system should keep the dc voltage across the capacitor constant and equal to the reference value, regardless of changes in the rotor speed and load.

1. INTRODUCTION

The demand for electrical energy is rapidly growing worldwide. On the other hand, fossil fuels resources will be depleted and the environmental pollution is inevitable which makes the mankind look for alternative energy resources. Besides, the renewable energy sources are promising solutions. Among these solutions, wind energy is the wide used one [1].

Squirrel cage type IG is widely used in wind power applications. Its capability to operate as a generator without external power supply allows its use in stand alone power generation systems without any reactive power from the grid. This interest is enhanced through its many advantages over other types of electric generators such as robustness, low price and maintenance free operation. In the case of stand alone operating, induction generators are usually excited by three ac capacitors connected across their stator terminals and then known as self excited induction generator (SEIG). This excitation method is the cheapest and simplest technique but it has several limitations. Indeed, the magnitude and frequency of the stator voltage are very sensitive to the variations of the rotation speed and the load. Different system configurations and control strategies are proposed in the literature in order to overcome these problems [2−5].

Among all control methods for SEIG, direct torque control (DTC) is considered particularly interesting being independent of machine rotor parameters. Its basic scheme is characterized by the absence of coordinate transformations, current regulators and PWM signals generators. It is simple, robust and allows a good torque control. However, the presence of hysteresis controllers for flux and torque lead to torque and current ripple and variable switching frequency for the PWM converter.

Vector control algorithms are also considered in SEIG power generating systems [2−5]. Generally, this control technique takes a cascaded configuration and four controllers are used (usually proportional integral (PI) controllers; external loops for the flux and the dc voltage control and inner loops for the currents control [3]. The switching signals for the PWM converter are then calculated using a PWM signal generator. In some cases, only two controllers are used for flux and dc voltage controls while the currents are controlled using hysteresis controllers [2, 5]. However, the use of hysteresis controllers leads to current ripple and variable switching frequency. In the other side, the use of four controllers leads to a complicated and bulky control scheme.

Note that a large number of solutions have been proposed in order to fulfill two main objectives: obtaining a precise and quick control of the flux and torque and reduction of the complexity of the algorithms involved in the vector control systems. In this paper, we propose a vector control strategy where the rotor flux and torque are controlled in a direct manner without resorting to the usually used current control loops. Only two control laws are used and synthesized by the sliding mode (SM) approach. The choice of this approach has been motivated by the presence of switches in the PWM converter. Changes in the state of the switches cause variation in the topology of the controlled system. As the SM is a variable structure controller, it is more suitable for systems with variable topology, which is the case of the studied system. In addition the sliding mode control is characterized by its robustness, high dynamic and it is insensitive to the system uncertainties [6, 7].

Usually, in conventional SEIG vector control systems, the non-linear behavior of the induction machine magnetic material is not taken into consideration, so the magnetizing inductance is kept constant [2]. However, it can leads to a serious problem of accuracy and reliability, even more in the cases where the reference of the flux is variable and the magnetic saturation occurs. Therefore, in order to get a more accurate prediction of the induction machine behavior and a good performance of the drive, and overcome the weakness of the involved estimators, the magnetic saturation phenomenon is taken into account in the dynamic model of the IG and updated online in the control system.

2. CONTROL STRUCTURE

The studied system, shown in Fig. 1, is constituted of a squirrel cage three-phase induction generator (IG) connected mechanically to a wind turbine through a gear box and

[1] Université de Bejaia, Faculté de Technologie, Laboratoire de Technologie Industrielle et de l'Information (LTII), 06000, Algérie, E-mail: aberbouradel@yahoo.fr, idjdarene@yahoo.fr.
[2] Université de Lille, Laboratoire d'Electrotechnique et d'Electronique de puissance (L2EP), 1, 59655, France, E-mail: mounaim.tounzi@univ-lille1.fr.

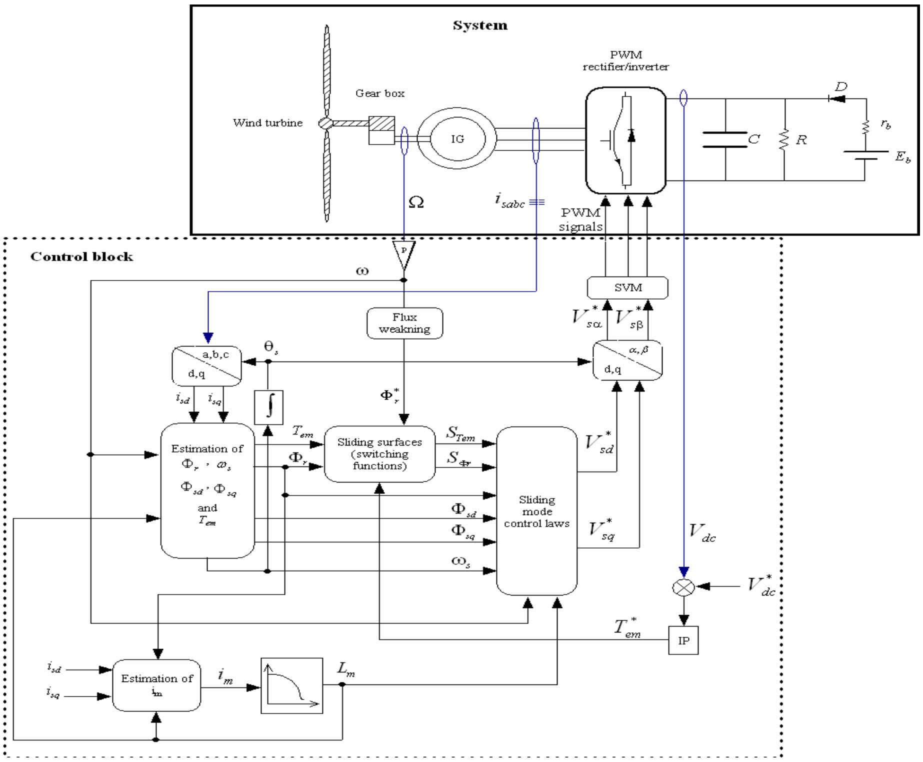

Fig. 1 – System and control scheme.

electrically to a PWM rectifier/inverter. The dc side of the latter is connected to a capacitor, a battery to start up the system if no remnant voltage is available and a diode which decouples the battery from the rectifier/inverter as soon as the dc voltage generated is higher than the one of the battery. The load R is equivalent to the global load seen from the dc side. The block diagram of the control scheme is also shown on the same figure.

2.1. INDUCTION MACHINE MODEL

Using stator and rotor fluxes as the state variables, the induction machine model can be written in the synchronous reference frame as follows:

$$\begin{bmatrix} \frac{d\Phi_{sd}}{dt} \\ \frac{d\Phi_{sq}}{dt} \\ \frac{d\Phi_{rd}}{dt} \\ \frac{d\Phi_{rq}}{dt} \end{bmatrix} = \begin{bmatrix} \frac{-1}{\sigma\tau_s} & \omega_s & \frac{L_m}{\sigma\tau_s L_r} & 0 \\ -\omega_s & \frac{-1}{\sigma\tau_s} & 0 & \frac{L_m}{\sigma\tau_s L_r} \\ \frac{L_m}{\sigma\tau_r L_s} & 0 & \frac{-1}{\sigma\tau_r} & (\omega_s-\omega) \\ 0 & \frac{L_m}{\sigma\tau_r L_s} & -(\omega_s-\omega) & \frac{-1}{\sigma\tau_r} \end{bmatrix} \begin{bmatrix} \Phi_{sd} \\ \Phi_{sq} \\ \Phi_{rd} \\ \Phi_{rq} \end{bmatrix} + \begin{bmatrix} V_{sd} \\ V_{sq} \\ 0 \\ 0 \end{bmatrix}, \quad (1)$$

where Φ_{sd}, Φ_{sq} and Φ_{rd}, Φ_{rq} are the d and q-axis stator and rotor flux components respectively. V_{sd} and V_{sq} are the d and q-axis stator voltage components. τ_s and τ_r are the stator and rotor time constants, with $\tau_s = L_s/R_s$ and $\tau_r = L_r/R_r$, R_s and R_r are stator and rotor resistances. L_s and L_r are the stator and rotor self inductances, L_m is the magnetising inductance. Besides, σ is the leakage coefficient with $\sigma = 1-L_m^2/(L_sL_r)$, ω_s and ω are the stator pulse and rotor speed expressed in electrical radians per second. The magnitude of the stator flux, rotor flux and stator voltage can be written as follows:

$$\begin{cases} \Phi_s = \sqrt{\Phi_{sd}^{\ 2} + \Phi_{sq}^{\ 2}} \\ \Phi_r = \sqrt{\Phi_{rd}^{\ 2} + \Phi_{rq}^{\ 2}}, \\ V_s = \sqrt{V_{sd}^{\ 2} + V_{sq}^{\ 2}} \end{cases} \quad (2)$$

where

$$\begin{cases} \Phi_{sd} = L_s i_{sd} + L_m i_{rd} \\ \Phi_{sq} = L_s i_{sq} + L_m i_{rq} \\ \Phi_{rd} = L_r i_{rd} + L_m i_{sd} \\ \Phi_{rq} = L_r i_{rq} + L_m i_{sq} \end{cases}. \quad (3)$$

We can also introduce the magnetizing current along the d and q-axis, such as:

$$\begin{cases} i_{md} = i_{sd} + i_{rd} \\ i_{mq} = i_{sq} + i_{rq} \end{cases} \quad \text{and} \quad i_m = \sqrt{i_{md}^2 + i_{mq}^2}. \quad (4)$$

To express L_m with respects to i_m, several approaches can be used whose simplest one is the polynomial approximation.

$$L_m = f\left(\left|i_m\right|\right) = \sum_{j=0}^{n} a_j \cdot \left|i_m\right|^j, \quad (5)$$

where a_j represent the polynomial's coefficients. The waveform of the magnetizing inductance is obtained through tests at no load for different voltage magnitudes. Figures 2a and 2b show a comparison between measur-ements and approximated values of a magnetizing inductance versus i_m.

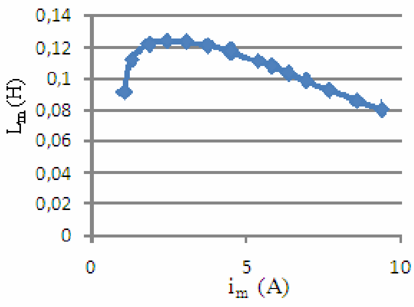

Fig. 2a – Magnetizing inductance *versus* magnetizing current (experimental).

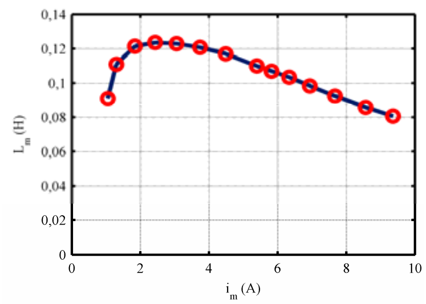

Fig. 2b – Magnetizing inductance *versus* magnetizing current (simulation).

2.2. DTRFC DESIGN USING SLIDING MODE APPROACH

According to the sliding mode theory, the first designing step consists in defining the switching functions (sliding surfaces). It is essential that the time derivatives of the switching functions depend directly on one of the variable inputs of the state model which are, in our case, the diphase stator voltage components V_{sd} and V_{sq}. Therefore, the switching functions of the rotor flux $S_{\Phi r}$ and electromagnetic torque S_{Tem} are defined as follows:

$$\begin{cases} S_{\Phi r} = k_{\Phi r}\left(\Phi_r^* - \Phi_r\right) + \dfrac{\mathrm{d}}{\mathrm{d}t}\left(\Phi_r^* - \Phi_r\right) \\ S_{Tem} = T_{em}^* - T_{em} \end{cases}, \tag{6}$$

where Φ_r^* and T_{em}^* are rotor flux and electromagnetic torque references respectively. The electromagnetic torque T_{em} is given as follows:

$$T_{em} = \frac{pL_m}{\sigma L_s L_r}\left(\Phi_{sq}\Phi_{rd} - \Phi_{sd}\Phi_{rq}\right), \tag{7}$$

$k_{\Phi r}$ is a positive coefficient. Its value is chosen by the designer, knowing that a high value of the latter leads to quick response of the rotor flux. The second step of the DTRFC design consists to find the global control law for each sliding surface. Its general formula is given as follows:

$$V = V_{eq} + V_n, \tag{8}$$

with V_{eq} is the so-called equivalent control voltage whose main rule is to maintain the controlled variable on the sliding surface but it is not intended to attract it toward the sliding surface, this task is devoted to the discontinuous control component V_n.

Note that, in the following we assume that the reference frame rotates at the speed of the rotor flux, so that, $\Phi_{rd} = \Phi_r$ and $\Phi_{rq}=0$, and the references derivative with respect to time are neglected. Therefore, by differentiating each sliding surface from (6) with respect to time and substituting corresponding relations from (1) yields:

$$\frac{\mathrm{d}S_{\Phi r}}{\mathrm{d}t} = -\frac{\mathrm{d}\Phi_r}{\mathrm{d}t}\left(k_{\Phi r} - \frac{1}{\sigma\tau_r}\right) + \frac{L_m}{\sigma\tau_s\tau_r}\left(R_s i_{sd} - \omega_s\Phi_{sq}\right) - \frac{L_m}{\sigma\tau_s\tau_r}V_{sd}, \tag{9}$$

$$\frac{\mathrm{d}S_{Tem}}{\mathrm{d}t} = \left(\frac{1}{\sigma\tau_s} + \frac{1}{\sigma\tau_r}\right)T_{em} + \frac{pL_m}{\sigma L_s L_r}\Phi_r\omega\Phi_{sd} - \frac{pL_m}{\sigma L_s L_r}\Phi_r V_{sq}. \tag{10}$$

The equivalent control law for each rotor flux and electromagnetic torque can be found by resolving the equations below:

$$\frac{\mathrm{d}S_{\Phi r}}{\mathrm{d}t} = 0 \quad \text{and} \quad \frac{\mathrm{d}S_{Tem}}{\mathrm{d}t} = 0. \tag{11}$$

Then, we obtain:

$$V_{sd\_eq} = -\frac{\sigma L_s\tau_r}{L_m}\frac{\mathrm{d}\Phi_r}{\mathrm{d}t}\left(k_{\Phi r} - \frac{1}{\sigma\tau_r}\right) + \frac{1}{\sigma\tau_s}\Phi_{sd} - \omega_s\Phi_{sq} - \frac{L_m}{\sigma L_r\tau_s}\Phi_r, \tag{12}$$

$$V_{sq\_eq} = \left(\frac{1}{\sigma\tau_s} + \frac{1}{\sigma\tau_r}\right)\Phi_{sq} + \omega\Phi_{sd}. \tag{13}$$

To find the complete voltage vector, the discontinuous term must be added to the equivalent control. It permits to control the concerned variable outside the sliding surface. Thus, the time derivatives of rotor flux and electromagnetic torque switching functions must be considered in the voltage vector formula, such as:

$$\begin{cases} V_{sd}^* = V_{sd\_eq} - \dfrac{\sigma L_s\tau_r}{L_m}\dfrac{\mathrm{d}S_{\Phi r}}{\mathrm{d}t} \\ V_{sq}^* = V_{sq\_eq} - \dfrac{\sigma L_s L_r}{pL_m\Phi_r}\dfrac{\mathrm{d}S_{Tem}}{\mathrm{d}t} \end{cases}, \tag{14}$$

with V_{sd}^* and V_{sq}^* are the global control law of rotor flux and electromagnetic torque respectively. The final step consists in finding a relationship, between the switching functions and their corresponding time derivatives, that allows attracting the rotor flux and electromagnetic torque toward the sliding surface. This relation is obtained by using a reaching condition [8], such as:

$$S_{\Phi r}\frac{\mathrm{d}S_{\Phi r}}{\mathrm{d}t} < 0 \quad \text{and} \quad S_{Tem}\frac{\mathrm{d}S_{Tem}}{\mathrm{d}t} < 0. \tag{15}$$

Then, the discontinuous control must be designed in such a way that permits to keep a different signs for the switching function and its derivative. So, the following choices are made:

$$\begin{cases} \dfrac{\mathrm{d}S_{\Phi r}}{\mathrm{d}t} = -g_{\Phi r}\,\mathrm{sign}\left(S_{\Phi r}\right) - c_{\Phi r}S_{\Phi r} \\ \dfrac{\mathrm{d}S_{Tem}}{\mathrm{d}t} = -g_{Tem}\,\mathrm{sign}\left(S_{Tem}\right) - c_{Tem}S_{Tem} \end{cases}. \tag{16}$$

Plugging corresponding relations from (16) into (14) leads to the DTRFC control laws below:

$$V_{sd}^{*} = V_{sd\_eq} - \frac{\sigma L_s \tau_r}{L_m}\left(-g_{\Phi r}\,\mathrm{sign}\left(S_{\Phi r}\right) - c_{\Phi r} S_{\Phi r}\right), \quad (17)$$

$$V_{sq}^{*} = V_{sq\_eq} - \frac{\sigma L_s L_r}{p L_m \Phi_r}\left(-g_{Tem}\,\mathrm{sign}\left(S_{Tem}\right) - c_{Tem} S_{Tem}\right). \quad (18)$$

The parameters ($g_{\Phi r}$ = 120 000, $c_{\Phi r}$ = 20 000, g_{Tem} = 500 000 and c_{Tem} = 20 000) are chosen optimally by observing the behavior of the controlled variables, based on criteria of high dynamic behavior and low ripples, *i.e.* the parameters choice has to be a good compromise between a small value which can lead to low torque dynamic and low ripples and a too high value which can lead to a high torque dynamic and high ripples.

Note that, in the case of this paper, the state variables are expressed in a reference frame rotating at the speed of the rotor flux, so that, Φ_{rd}= Φ_r and Φ_{rq}=0. Therefore, the usually used estimators in the conventional flux oriented control are also valid in the studied strategy. The rotor flux, electromagnetic torque, the synchronous frequency and the stator flux components can be estimated as follows [2]:

$$\begin{gathered}\Phi_r = \frac{L_m i_{sd}}{1+\tau_r s},\quad T_{em} = p\frac{L_m}{L_r}\Phi_r i_{sq},\quad \omega_s = \frac{L_m i_{sq}}{\tau_r \Phi_r} + p\ \ \Omega \\ \Phi_{sd} = \sigma L_s i_{sd} + \frac{L_m}{L_r}\Phi_r \quad \text{and} \quad \Phi_{sq} = \sigma L_s i_{sq}\end{gathered}, \quad (19)$$

where s is the time derivative operator. As can be seen from (19), all the estimators depend on the magnetizing inductance. Then, the fact of considering it constant can leads to serious problem of accuracy. Hence, in order to get a good performance of the drive, the magnetizing inductance is updated online in the controller. The accuracy can be improved more by adding the non-linear behavior of the rotor resistance with respect to the temperature, indeed, Φ_r, Φ_{sd} and ω_s depend on the rotor time constant. But this is not within the scope of this paper.

3. SIMULATION RESULTS

The logic control signals of the PWM converter are calculated by using the space vector modulation (SVM) technique. The details about its implementation can be found in [9]. The nominal parameters of the induction machine are listed in the appendix. In this paper, the dc voltage reference value is put equal to V_{dc}^{*} = 570 V. This will lead us to an rms voltage of about 230 V in the ac side. The reference rotor flux is inversely proportional to the speed (flux weakening mode):

$$\Phi_r^{*} = \frac{\omega_{rat}}{\omega}\Phi_{r\_rat}, \quad (20)$$

where, $\Phi_{r\text{-}rat}$ and ω_{rat} are the rated rotor flux ($\Phi_{r\text{-}rat}\approx$ 0.7 Wb) and synchronous speed, respectively. This strategy would allow avoiding a high saturation of the structure when the rotation speed is beyond the synchronous speed. Note that, a limitation must be imposed to the controlled rotor flux in order to avoid high saturation level when the speed is weak, as can be deduced from (20).

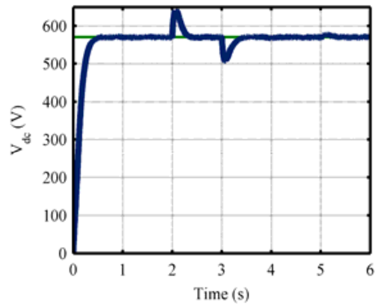

Fig. 3 – Dc voltage.

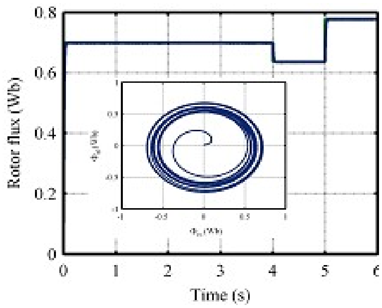

Fig. 4 – Rotor flux.

The value of the load resistance R is initially equal to 70 Ω which is the value that allows the machine to generate a significant power related to the operating conditions. At t = 2 s the resistance is increased to R = 100 Ω, then it is decreased to its initial value at t = 3 s. The rotation speed is initially kept at its synchronous speed (750 rpm). A step increment of 10 % is done at t = 4 s. Then at t = 5 s, a step decrease of 20 % is applied.

Figure 3 shows the time waveform of the dc voltage that is well controlled. As can be seen, the dc voltage is much more sensitive to load disturbances than speed disturbances. Figure 4 shows the rotor flux response. It is well controlled and shows a very quick response obtained for $K_{\Phi r}$ = 100. In the same figure, we also show the rotor flux locus in the α-β reference frame. Figure 5 shows the electromagnetic torque time waveform. It tracks very well its reference value. We can also observe the impact of the load and rotation speed variations on the electromagnetic torque. Fig 6 shows the sliding surface of the rotor flux and electromagnetic torque. As can be seen, they are both forced to zero. Finally, Figs. 7 and 8 show the magnetizing current time and the value of the magnetizing inductance obtained for the considered operation As this inductance depends on the magnetic saturation level, we can note the influence of the load variations at t = 2 s and t = 3 s. This can be directly linked to the magnetizing current i_m variations (Fig. 7). At t = 4 s, the magnetizing inductance increases due to the decrease of the rotor flux which is imposed by the increase of the speed at constant load. The inverse effect is obviously observed at t = 5 s.

4. CONCLUSIONS

In this paper, DTRFC based on vector control concept and synthesized by the sliding mode approach of an autonomous induction generator is studied. This strategy permits a direct control of flux and torque without resorting to the usually used current control loop. Thus, the complexity of the controller is reduced. In addition, the

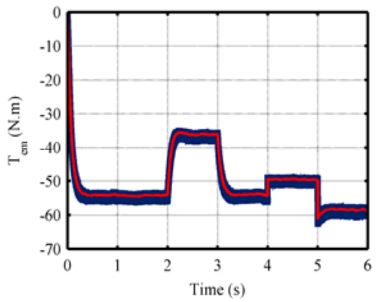

Fig. 5 – Electromagnetic torque.

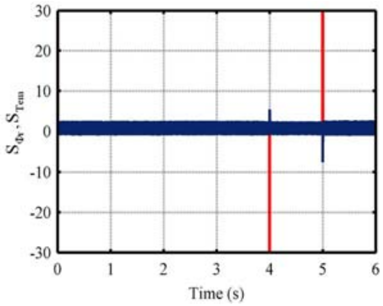

Fig. 6 – Sliding surfaces.

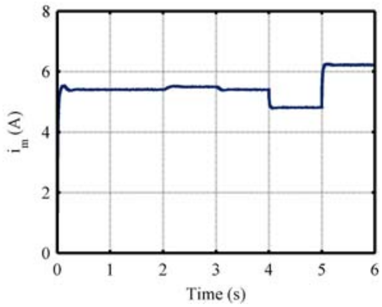

Fig. 7 – Magnetizing current.

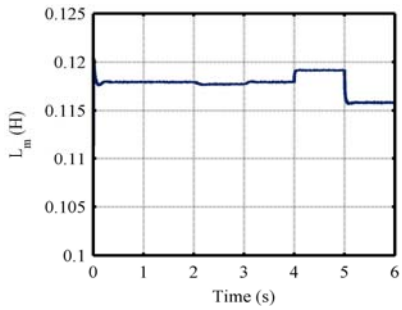

Fig. 8 – Magnetizing inductance.

adaptation of the magnetizing inductance permits to avoid the weakness of the involved estimators. Finally, the simulation results showed the effectiveness of the proposed DTRFC strategy, so it can be considered as a promising alternative to the existing solutions in the field of renewable wind energy systems.

APPENDIX

Parameters of the induction machine:

$P_N = 5.5$ kW, $U_N = 230/400$ V, $I_N = 23.8/13.7$ A, 50 Hz, $\Omega_N = 690$ rpm, $J = 0.230$ kg.m^2, $d = 0.0025$ N.m rad·s^{-1}, $R_s = 1.07131\ \Omega$, $R_r = 1.29511\ \Omega$, $p = 4$.

Received on July 23, 2015

REFERENCES

1. M. Cheng, Y. Zhu, *The state of the art of wind energy conversion systems and technologies*: A review, Energy Conversion and Management, **88**, pp. 332–347, 2014.
2. K. Idjdarene, D. Rekioua, T. Rekioua, A. Tounzi, *Vector control of autonomous induction generator taking saturation effect into account*, Energy Conversion and Management, **49**, pp. 2609–2617, 2008.
3. D. Seyoum, C. Grantham, T*erminal voltage control of a wind turbine driven isolated induction generator using stator oriented field control*, IEEE transactions on industrial Applications, 2003, pp. 846–852.
4. S. Hammadi, N. Hidouri, L. Sbita, *A DTC SEIG drive scheme for an isolated wind turbine buck system*, International Conference on Control, Decision and Information Technologies (CoDIT'13), 2013, pp. 543–548.
5. M. Bašić, D. Vukadinović, M. Polić, *Fuzzy DC-voltage controller for a vector controlled stand-alone induction generator*, International Journal Of Circuits, Systems And Signal Processing, **7**, *3*, pp. 181–190, 2013.
6. A. Kerboua, M. Abid, *Hybrid fuzzy siliding mode control of a doubly-fed induction generator in wind turbines*, Rev. Roum. Sci. Techn. – Électrotechn. et Énerg., **57**, *4*, pp. 412–421, 2012.
7. A. Boucheta, I.K. Bousserhane, A. Hazzab, B. Mazari, M.K. Fellah, *Fuzzy-silding mode controller for linear induction motor control*, Rev. Roum. Sci. Techn. – Électrotechn. et Énerg., **54**, *4*, pp. 405–414, 2009.
8. M. Adjoudj, M. Abid, A. Aissaoui, Y. Ramdani, H. Bounoua, *Sliding mode control of a doubly fed induction generator for wind turbines*, Rev. Roum. Sci. Techn. – Électrotechn. et Énerg., **56**, *1*, pp. 15–24, 2011.
9. T.J. Fu, W.F. Xie, *A novel sliding-mode control of induction motor using space vector modulation technique*, ISA Transactions, **44**, pp. 481–490, 2005.